Virology 443 (2013) 363–374

Contents lists available at SciVerse ScienceDirect

Virology

journal homepage: www.elsevier.com/locate/yviro

The P6 protein of *Cauliflower mosaic virus* interacts with CHUP1, a plant protein which moves chloroplasts on actin microfilaments

Carlos A. Angel [a], Lindy Lutz [c], Xiaohua Yang [b], Andres Rodriguez [a], Adam Adair [a], Yu Zhang [a], Scott M. Leisner [c], Richard S. Nelson [b], James E. Schoelz [a,*]

[a] Division of Plant Sciences, University of Missouri, Columbia, MO 65211, USA
[b] The Division of Plant Biology, The Samuel Roberts Noble Foundation, Ardmore OK 73401, USA
[c] Department of Biological Sciences, University of Toledo, Toledo OH 43606, USA

ARTICLE INFO

Article history:
Received 11 February 2013
Returned to author for revisions
11 March 2013
Accepted 18 May 2013
Available online 12 June 2013

Keywords:
Intracellular movement
Subcellular localization
Inclusion bodies
CaMV

ABSTRACT

The gene VI product, protein 6 (P6), of *Cauliflower mosaic virus* (CaMV) assembles into large, amorphous inclusion bodies (IBs) that are considered sites for viral protein synthesis and viral genome replication and encapsidation. P6 IBs align with microfilaments and require them for intracellular trafficking, a result implying that P6 IBs function to move virus complexes or virions within the cell to support virus physiology. Through a yeast two-hybrid screen we determined that CHUP1, a plant protein allowing chloroplast transport through an interaction with chloroplast and microfilament, interacts with P6. The interaction between CHUP1 and P6 was confirmed through colocalization *in vivo* and co-immunoprecipitation assays. A truncated CHUP1 fused with enhanced cyan fluorescent protein, unable to transport chloroplasts, inhibited intracellular movement of P6–Venus inclusions. Silencing of CHUP1 in *N. edwardsonii* impaired the ability of CaMV to infect plants. The findings suggest that CHUP1 supports CaMV infection through an interaction with P6.

Introduction

Plant viruses have at least three distinct activities necessary to complete their disease cycle in a host: those required to replicate, encapsidate, and move the virus throughout the plant. Some plant viruses encode additional proteins with functions dedicated to vector transmission or defeating plant defenses, but it is generally accepted that the genomic capacity of plant viruses is small, with an upper limit of perhaps 15–20 proteins. To overcome their limited coding capacity, it is likely that each viral protein has multiple functions and contacts with host factors. Collectively these functions and interactions determine the outcome of the infection.

The P6 protein of *Cauliflower mosaic virus* (CaMV) is an example of a plant virus protein with multiple functions and interactions. P6 functions to support the synthesis of viral proteins from the 35S viral RNA, suppresses gene silencing, and inhibits SA-mediated plant defenses (Hohn and Fütterer, 1997; Love et al., 2007, 2012; Park et al., 2001). In addition, P6 functions as an avirulence determinant in some solanaceous and cruciferous species, and is a chlorosis symptom determinant in susceptible hosts (Baughman et al., 1988; Daubert et al., 1984; Hapiak et al., 2008; Schoelz et al., 1986). P6 is the most abundant protein component of the amorphous, electron dense inclusion bodies (IBs) present during virus infection (Odell and Howell, 1980; Shockey et al., 1980). P6-containing IBs induced during virus infection are likely "virion factories", as they are the primary site for CaMV protein synthesis, genome replication, and assembly of virions (Hohn and Fütterer, 1997). P6 physically interacts with the CaMV capsid (P4) and movement (P1) proteins, as well as the two viral proteins necessary for insect transmission (P2 and P3) (Hapiak et al., 2008; Himmelbach et al., 1996; Lutz et al., 2012; Ryabova et al., 2002).

Recently, a new function for P6 was suggested when it was shown that P6 IBs induced by ectopic expression of P6 associate with actin microfilaments, microtubules and the endoplasmic reticulum, and were capable of intracellular movement along microfilaments (Harries et al., 2009a). Furthermore, latrunculin B, a pharmacological agent that disrupts microfilaments by preventing polymerization of actin monomers, abolished CaMV local lesion formation in *N. edwardsonii*, an indication that intact microfilaments are essential for CaMV infections (Harries et al., 2009a). Collectively, these experiments suggested that P6 IBs might be responsible for intracellular trafficking of virions to plasmodesmata, in addition to the role of the P6 protein in translation of the 35S RNA and gene silencing suppression.

Prior to the report by Harries et al. (2009a), the P6 protein of CaMV had not been considered to have a role in CaMV movement,

* Corresponding author. Fax: +1 573 882 0588.
E-mail address: schoelzj@missouri.edu (J.E. Schoelz).

0042-6822/$ - see front matter © 2013 Elsevier Inc. All rights reserved.
http://dx.doi.org/10.1016/j.virol.2013.05.028

but there was evidence suggesting its function in this activity. CaMV virions move from cell to cell through plasmodesmata modified into tubules through the function of its movement protein, P1 (Kasteel et al., 1996; Perbal et al., 1993). However, it is unlikely that the CaMV P1 protein transports the virions to the plasmodesmata since P1 does not appear to directly interact with the virion. The CaMV P3 protein does interact with virions through the formation of a tetrameric structure anchored into the virions (Leclerc et al., 1998, 2001). Electron microscopy studies have indicated that P1 and P3 colocalize with virions only within the plasmodesmata, and it has been suggested that the P3/virion complex travels to the plasmodesmata independently from P1 (Stavolone et al., 2005). Consequently, there is a need for a second CaMV protein to fulfill the role of intracellular transport. Since P6-containing IBs are the site for virion accumulation and they are capable of movement, they may be responsible for delivering virions to CaMV P1 located at the plasmodesmata (Harries et al., 2009a; Schoelz et al., 2011). At the very least, there must be a mechanism that would account for the transfer of CaMV virions from the P6 IBs to the plasmodesmata.

In this study we utilized a yeast two-hybrid assay to identify host proteins that interact with CaMV P6. We show here that P6 physically interacts with CHUP1 (Chloroplast Unusual Positioning 1), a protein which is encoded by a single gene in Arabidopsis and is localized to the outer membrane of chloroplasts (Oikawa et al., 2003, 2008). A CHUP1-ECFP (Enhanced Cyan Fluorescent Protein) fusion protein was observed to relocate a P6-Venus fusion protein to chloroplasts *in vivo*. An interaction between CHUP1 and P6 also was demonstrated through co-immunoprecipitation studies from plant extracts. Overexpression of a truncated CHUP1 in a transient expression assay in *N. benthamiana* blocked the movement of P6 IBs. This observation was correlated with a delayed rate of CaMV local lesion development when CHUP1 was silenced in *N. edwardsonii*. Our data provide an explanation for the subcellular localization of P6 IBs to, and movement along, microfilaments. In addition our data provide further evidence that a complex composed of P6 and virions may contribute to intracellular movement of CaMV particles necessary to infect the host.

Results

A yeast two-hybrid screen reveals that the CaMV P6 protein interacts with CHUP1

Previous studies showed that CaMV P6 interacts with the ribosomal proteins L13, L18, and L24, along with eukaryotic translation factor 3 subunit g (eIF3g) (Bureau et al., 2004; Leh et al., 2000; Park et al., 2001), consistent with the role of P6 in re-initiation of translation of the polycistronic 35S mRNA. P6 also interacts with the RNA silencing protein DRB4 (Haas et al., 2008), which is consistent with the role of P6 as a silencing suppressor. To identify additional proteins that interact with CaMV P6, a yeast two-hybrid screen of an *A. thaliana* cDNA library composed of transcripts representing one-week old seedlings was performed by Hybrigenics Services (Paris, France). The bait consisted of the full-length sequence of P6 of CaMV strain W260 (Wintermantel et al., 1993). Of the 85 Arabidopsis clones found in this screen, 17 were identified as eIF3g. None of the other proteins previously shown to interact with P6 (e.g. L13, L18, L24 or DRB4) appeared in this Y2H screen. Nonetheless, the result with eIF3g demonstrates the capacity of our screen to identify host proteins previously shown to interact with P6 through two-hybrid screens (Park et al., 2001).

One of the additional clones selected in the Hybrigenics screen was identified as CHUP1 (*At3G25690*), a unique Arabidopsis gene encoding a protein that localizes to the outer membrane of chloroplasts (Oikawa et al., 2003). Previously it was shown that CHUP1 has four important functional domains (Fig. 1A). The N-terminus contains a hydrophobic domain that targets CHUP1 to the chloroplast outer envelope. A second domain is a coiled-coil motif that interacts with the plasma membrane, permitting CHUP1 to serve as a bridge to anchor chloroplasts to plasma membranes along the cell wall, and also is important for homo-dimerization of the protein. A third domain binds to F-actin both *in vitro* and *in vivo*, and a fourth proline-rich domain interacts with profilin and actin. In addition, there are two embedded leucine-zipper motifs, one in the coiled-coil region and the other downstream from the proline-rich region, each of which may be important for intramolecular interactions. (Oikawa et al., 2003, 2008; Lehmann et al., 2011; Schmidt von Braun and Schleiff, 2008). In the Hybrigenics yeast two hybrid assay, CaMV P6 was shown to interact with the coiled-coil region of CHUP1 (Fig. 1A).

To identify the specific region(s) of P6 that interact with CHUP1, a second yeast two-hybrid assay was performed. Four domains of P6, previously investigated for their role in self-association (D1–D4; Fig. 1A) (Li and Leisner, 2002), were used as bait for CHUP1. Yeast cells co-transformed with the full length P6 fused to the LexA DNA-binding domain in the pEG202 plasmid and a portion of the coiled-coil domain of CHUP1 fused to the B42

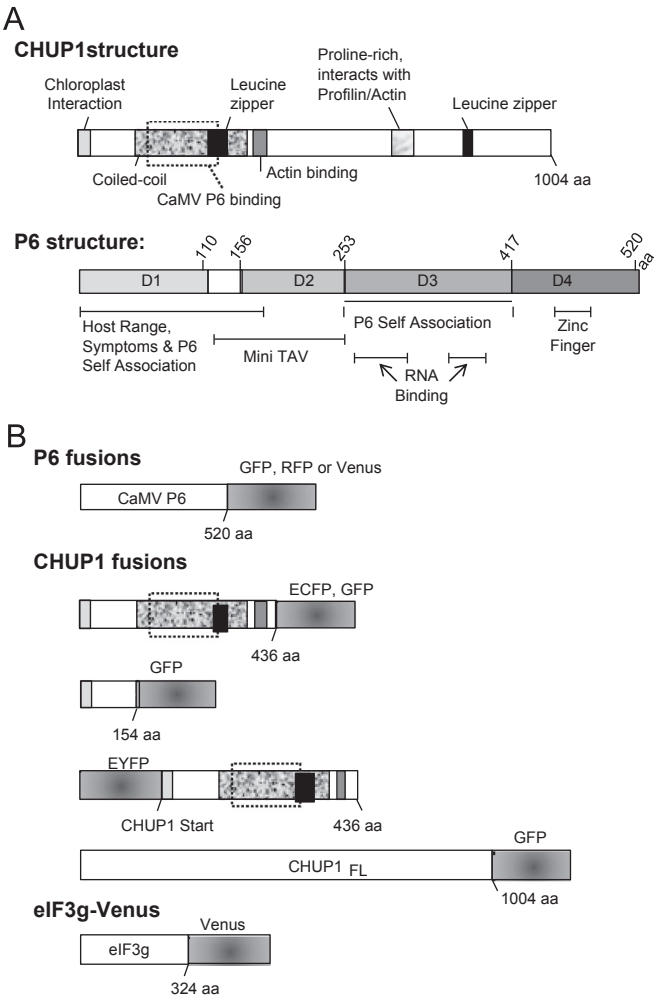

Fig. 1. CHUP1, P6 and eIF3g constructs used for confocal microscopy or co-immunoprecipitation. (A) Structure of CHUP1 and CaMV P6 proteins. The functions of P6 domains D1–D4 tested for self interaction (Li and Leisner, 2002) and interaction with a portion of CHUP1. The mini TAV is the minimal region for the translational transactivation function. The functions of CHUP1 domains are shown below. (B) Structure of P6, CHUP1, eIF3g fusions developed for confocal microscopy.

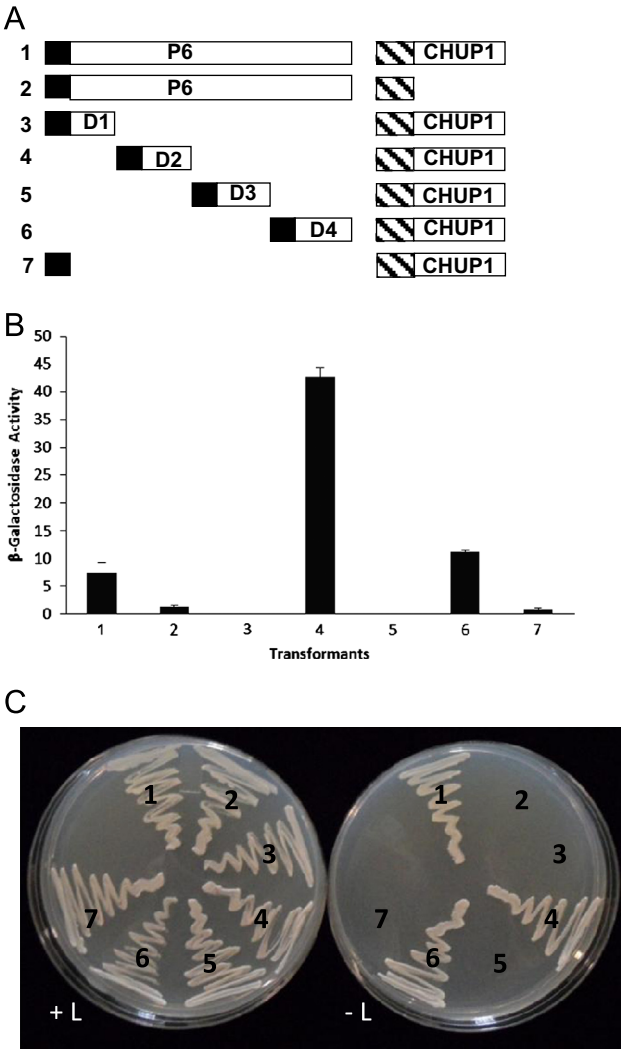

Fig. 2. Interaction of CaMV P6 and CHUP1 proteins in yeast two-hybrid screens. (A) Full-length CaMV P6 and P6 domains were screened for interaction with the 363 nt sequence of CHUP1 protein originally identified in the Hybrigenics screen. The black boxes indicate the LexA DNA-binding domain of the yeast vector pEG202 and the hatched boxes indicate B24 activation domain present in the yeast plasmid pJG4. (B) β-galactosidase activity of yeast transformants expressing the constructs illustrated in panel A. (C) Growth of yeast transformants on media with (left) and without (right) leucine.

activation domain in the pJG4-5 plasmid showed leucine-independent growth and β-galactosidase activity (Fig. 2). Similarly, the four P6 domains necessary for self-association were each independently fused to the LexA DNA-binding domain and co-transformed with the B42–CHUP1 fusion. Yeast co-transformed with either domains D2 or D4 and CHUP1 grew on leucine-deficient media and the highest level of β-galactosidase activity, indicating a strong interaction, was observed with the D2–CHUP1 combination (Fig. 2). Interestingly, no interaction was detected between domains D3 or D1 with CHUP1. Since domain D3 was shown previously to interact with eIF3g and L24 (Park et al., 2001), our results show that host proteins interact with different domains within P6.

Validation of co-localization studies with CaMV P6 and eIF3g

Although P6 has been shown to associate with plant proteins and with itself, these interactions have not been visualized through co-localization studies in live cells. As a prerequisite for evaluating co-localization of CHUP1 with P6 *in vivo*, we first sought to establish, as a standard, the co-localization of P6 with itself and with eIF3g. By fusing the green fluorescent protein (GFP) to the C-terminus of P6, it was possible to image amorphous IBs in live, infected cells (Harries et al., 2009a). To visualize P6-P6 associations *in vivo*, we co-agroinfiltrated P6–GFP with P6–RFP (Campbell et al., 2004; Heim and Tsien, 1996). Of the 38 P6–GFP IBs and 40 P6–RFP IBs that we counted, we found that GFP and RFP signals co-localized in 79% of the IBs (Fig. 3A–C). To visualize the localization of eIF3g in cells individually and in the presence of P6, a full-length eIF3g cDNA from *A. thaliana* was fused to a sequence encoding the yellow fluorescent protein Venus (Venus) (Nagai et al., 2002). *N. benthamiana* leaf sections agroinfiltrated with only eIF3g–Venus contained numerous small, aggregates distributed within the cytoplasm (Fig. 3D and E). Upon co-agroinfiltration of eIF3g–Venus with P6–RFP, the eIF3g–Venus signal was relocated to and concentrated within the P6–RFP inclusion bodies (Fig. 3F–H). This result and those from earlier studies showing that ribosomes appeared to aggregate around IBs in CaMV-infected Chinese Cabbage leaves (Conti et al., 1972) together support the conclusion that translation occurs in the vicinity of the IBs.

CHUP1 and CaMV P6 co-localize in vivo

To examine the influence of CHUP1 on the subcellular localization of P6, we generated a cDNA clone consisting of the first 436 codons for *A. thaliana* CHUP1 fused to the 5′ end of ECFP (enhanced *cyan fluorescent protein*) coding sequence (Fig. 1B) (Heim and Tsien, 1996). This CHUP1 fusion, $CHUP1_{436}$–ECFP, was similar in composition to a clone ($CHUP1_{1–500}$–GFP) previously shown to interact with actin, to be targeted to the chloroplast outer envelope, and to associate with the plasma membrane (Oikawa et al., 2003, 2008). Upon agroinfiltration of $CHUP1_{436}$–ECFP into leaf sections of *N. benthamiana*, the ECFP signal was observed in a band that surrounded chloroplasts (Fig. 4A–C), in agreement with findings from previous studies (Oikawa et al., 2003, 2008). In addition, the ectopic expression of $CHUP1_{436}$–ECFP caused chloroplasts to aggregate (Fig. 4B). To visualize P6 in live cells in this study, we fused Venus to the C-terminus of the CaMV strain W260 P6 coding sequence and the construct was agroinfiltrated into *N. benthamiana* leaf panels. In agreement with a previous study (Harries et al., 2009a), CaMV P6–Venus IBs in the absence of additional ectopically expressed CHUP1, were well-defined, but they were not specifically associated with chloroplasts (Fig. 4D–F).

Co-agroinfiltration of $CHUP1_{436}$–ECFP with P6–Venus revealed that these proteins consistently co-localized in cells. Upon co-agroinfiltration, the $CHUP1_{436}$–ECFP fusion was associated with and surrounded chloroplasts, as observed previously when expressed in the absence of P6–Venus (compare Fig. 4A with G). Two patterns were associated with the P6–Venus signal during co-agroinfiltration. In one pattern, signal representing P6–Venus was observed surrounding chloroplasts, reminiscent of the $CHUP1_{436}$–ECFP pattern (Fig. 4G–J), in addition to being more diffuse and distributed over a larger area than when infiltrated by itself. In the second pattern, the P6–Venus formed compact IBs embedded in a CHUP1 matrix (Suppl. Fig. 1). To examine whether the co-localization of CHUP1 with P6 was dependent on the coiled-coil domain of CHUP1, as indicated in the yeast two-hybrid screen, we eliminated the portion of the coiled-coil domain that contained the P6 binding region (Suppl. Fig. 4) to create $CHUP_{154}$–GFP. Agroinfiltation of $CHUP1_{154}$–GFP into *N. benthamiana* leaf tissue revealed that it retained the capacity for localization to the chloroplast outer membrane (Suppl. Fig. 2A–C). Furthermore, expression of $CHUP_{154}$–GFP caused the chloroplasts to aggregate, similar to the $CHUP1_{436}$–ECFP construct. Co-agroinfiltration of $CHUP1_{154}$–GFP with P6–RFP showed that the capacity for co-localization of the two proteins was abolished (Suppl. Fig. 2D–F). This experiment confirmed that the coiled-coil domain of CHUP1 was necessary for its association with P6.

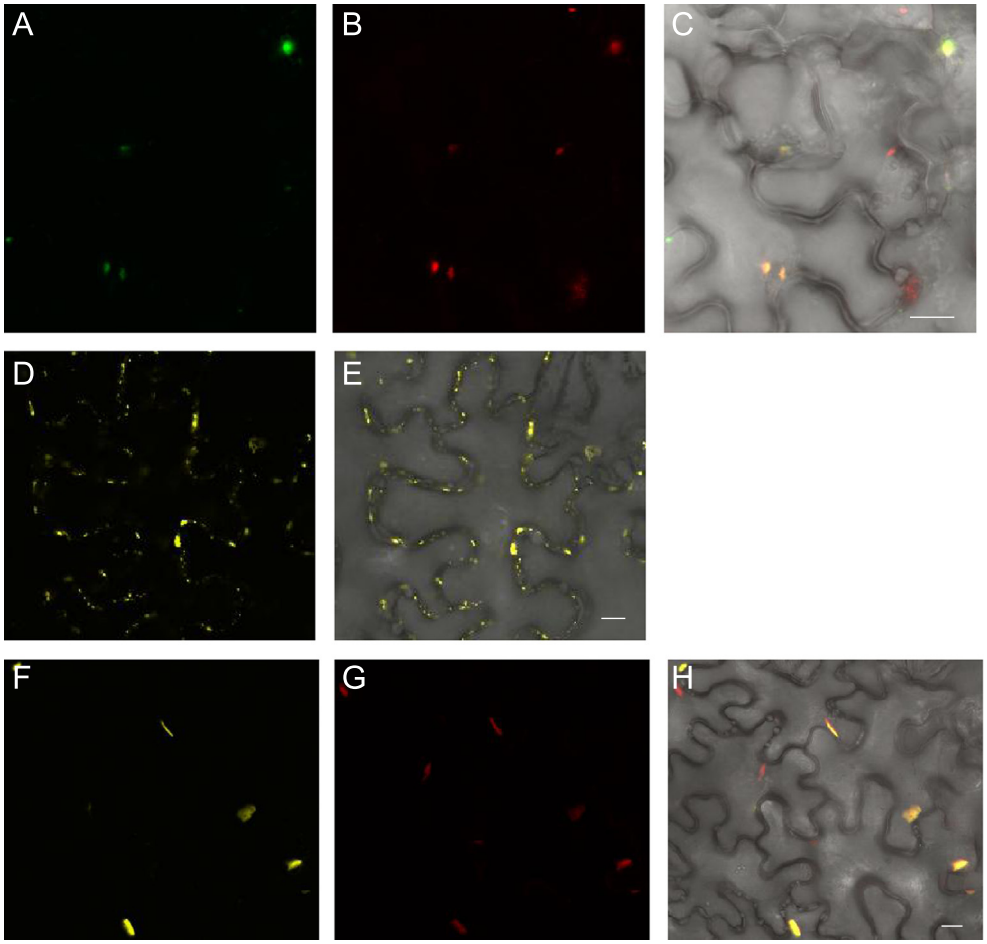

Fig. 3. Colocalization of CaMV P6–GFP, P6–RFP, and eIF3g–Venus in *N. benthamiana* leaves by confocal microscopy. (A) Expression at 4 dpinf of P6–GFP. (B) Expression at 4 dpi of P6-RFP in the same cells as A. (C) Overlay of panels A and B. (D) Expression of eIF3g–Venus alone, at 3 dpi. (E) Bright field overlay of D. (F) Expression of eIF3g–Venus at 4 dpinf. (G) Expression of P6–RFP in the same cells as F. (H) Overlay of panels E and F with brightfield image. Magnification bar is 10 μm.

To examine whether the full length CHUP1 would co-localize with CaMV P6 *in vivo*, a full length CHUP1 gene with GFP fused to the 3′ end (CHUP1$_{FL}$–GFP) (Fig. 1) was obtained from Dr. Sam-Geun Kong (Kyushu University). Upon co-bombardment of *N. benthamiana* leaves with CHUP$_{FL}$–GFP and P6–RFP, the CHUP1$_{FL}$–GFP was associated with chloroplasts (Fig. 5A and C), as reported by Oikawa et al. (2003, 2008). In this image, a compact P6-RFP IB co-localized with the CHUP1$_{FL}$–GFP protein and was adjacent to a chloroplast, and P6-RFP signal was also present in a more diffuse pattern that overlapped with the CHUP1$_{FL}$–GFP signal surrounding each of the chloroplasts (Fig. 5B and D). Therefore, CHUP1$_{FL}$–GFP co-localized with P6–RFP, similar to the results obtained with CHUP1$_{436}$–ECFP.

P6–RFP Is co-immunoprecipitated with P6-GFP and CHUP1$_{436}$-GFP

To develop a standard for co-immunoprecipitation of proteins that interact with P6, we co-agroinfiltrated P6–RFP with P6–GFP, as the self-aggregating properties of this protein have been well established, both in a yeast two-hybrid assay (Li and Leisner, 2002) and *in vivo* (Fig. 3A–C). Both P6–GFP and P6–RFP were readily detected by western blot in agroinfiltrated tissues when expressed individually (Fig. 6A and B, lanes 3 and 4) or when co-expressed (Fig. 6A and B, lane 6). Furthermore, antibodies to RFP and GFP did not cross react with each other at levels that would influence IP results (Fig. 6A and B). In a previous study we found that P6 is partially processed into smaller protein products (Yu et al., 2003). The processing of P6–GFP and P6–RFP into smaller protein products was largely blocked through the addition of protease and phosphatase inhibitors, including PMSF, Na_3VO4 and NaF, although even in the presence of these inhibitors a smaller band was visible in the western blot for P6–RFP (Fig. 6B).

To investigate the interaction of P6 with itself and with CHUP1 during immunoprecipitation analyses, plant tissue extracts co-agroinfiltrated with either P6–GFP/P6–RFP or CHUP1$_{436}$–GFP/P6–RFP were incubated with GFP antibodies immobilized onto sepharose beads. Following extensive washes, the bound proteins were eluted from the beads, separated by gel electrophoresis, blotted onto a nitrocellulose membrane, and probed with antibodies to RFP. The full-length P6–RFP protein and a smaller processed product were detected upon co-immunoprecipitation with P6–GFP (Fig. 6C, lane 6) or CHUP1$_{436}$-GFP (Fig. 6C, lane 5), but were not detected when P6–GFP was omitted from the co-immunoprecipitation assay (Fig. 6C, lane 4). As an additional negative control for the co-immunoprecipitation of P6, plant tissue extracts containing P6–GFP and P6–RFP were incubated with FLAG-M2 antibodies immobilized onto sepharose beads. In this assay, P6–RFP was not co-immunoprecipitated, as revealed in a western blot with RFP antibodies (data not shown), confirming that detection of P6–RFP depends on the immunoprecipitation of CHUP$_{436}$–GFP or P6–GFP. We concluded that the co-immunoprecipitation assay detected a P6–CHUP1$_{436}$ interaction with equivalent sensitivity as a P6–P6 interaction.

P6 and chloroplast targeting signals in CHUP1 do not overlap

A previous study had shown that fusion of GFP to the N-terminus of CHUP1 blocked its interaction with chloroplasts (Oikawa et al., 2008). The presence of GFP was proposed to mask

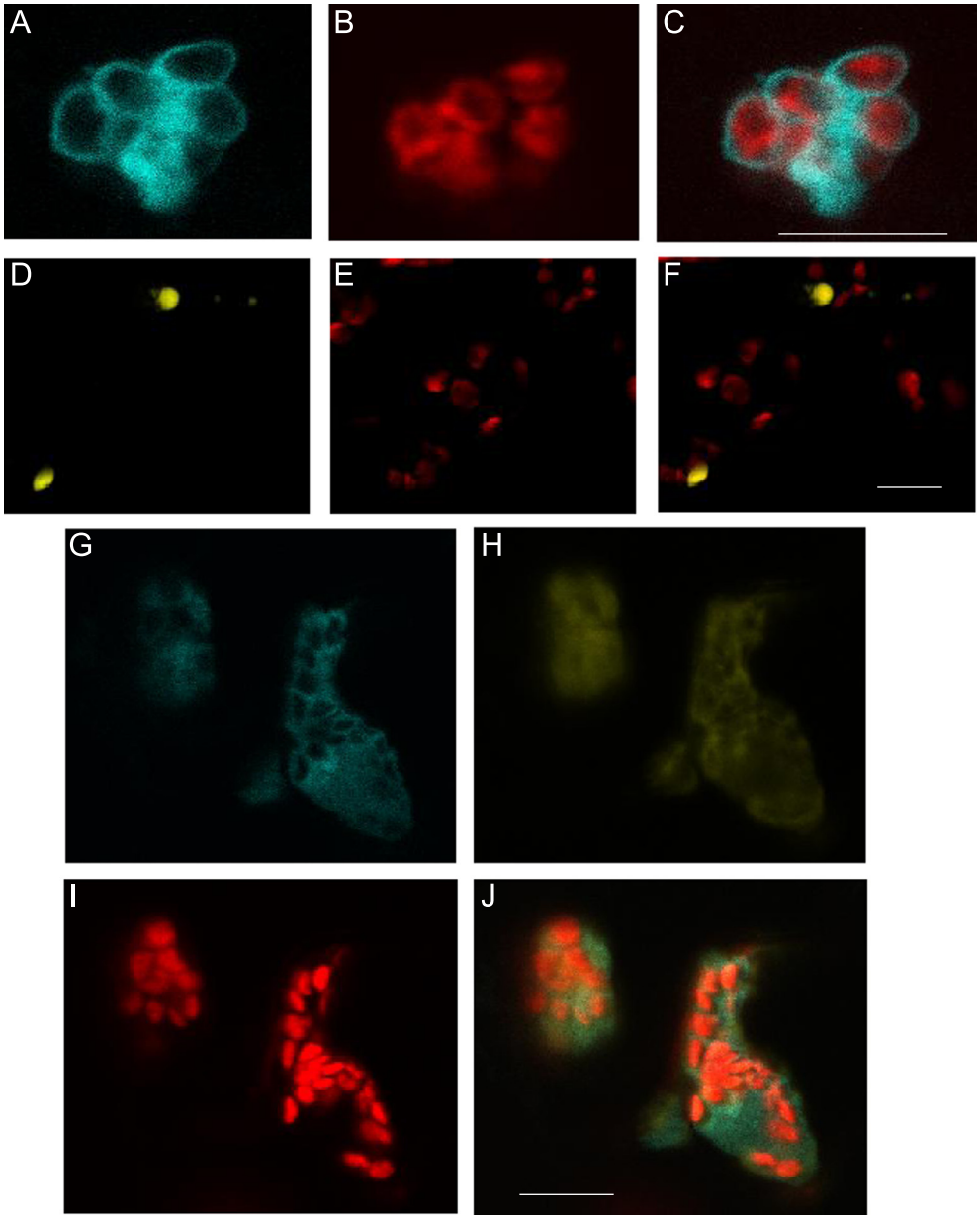

Fig. 4. Colocalization of CaMV P6–Venus with CHUP1$_{436}$–ECFP in *N. benthamiana* leaf cells by confocal microscopy. (A) Expression of CHUP1$_{436}$–ECFP. (B) Autofluorescence of chloroplasts present in the image shown in panel A. (C) Overlay of panels A and B. (D) Expression of P6–Venus. (E) Autofluorescence of chloroplasts present in the image shown in panel D. (F) Overlay of panels D and E. (G–J) co-expression of CHUP1$_{436}$–ECFP and CaMV P6–Venus in the same cells. (G) Expression of CHUP1$_{436}$–ECFP. (H) Expression of P6–Venus in the image shown in panel G. (I) Autofluorescence of chloroplasts present in the image shown in panel G. (J) Overlay of panels G–I. Magnification bars = 10 μm.

the chloroplast targeting sequence of CHUP1 present on its N-terminus. To determine whether the stearic hindrance of the chloroplast-targeting signal would affect the interaction of CHUP1 and P6, we fused EYFP (Baird et al., 1999) to the N-terminus of CHUP1$_{436}$ and evaluated its interaction with P6-RFP (Fig. 1B). In agreement with previous results for the 500 aa CHUP1 fragment (Oikawa et al., 2008), the EYFP–CHUP1$_{436}$ protein was detected in the cytosol, including trans-cellular cytosolic connections. In particular, the EYFP–CHUP1$_{436}$ protein was not located to the outer membrane of chloroplasts (Fig. 7A–C). Interestingly, when EYFP–CHUP1$_{436}$ was co-agroinfiltrated with P6–RFP, the CHUP1$_{436}$ protein was relocated from the cytosol to the P6 inclusion bodies. Due to the different emission frequencies of RFP and the auto-fluorescing chloroplasts, the P6 inclusion bodies could be distinguished from chloroplasts (Fig. 7E and F), and CHUP1$_{436}$ was clearly associated with the former and not the latter (Fig. 7D–G). This finding indicates that the CHUP1 domain responsible for binding P6 does not overlap with the chloroplast binding domain. The contrast in the results presented in Figs. 4 and 7 illustrate the modular nature of the association of CHUP1 with P6 and chloroplasts.

A truncated CHUP1–ECFP protein acts as a dominant negative inhibitor of P6 inclusion body movement

When CHUP1$_{1–500}$–GFP was introduced into *chup1* Arabidopsis plants, chloroplasts were found along the anticlinal cell walls at all light intensities examined (Oikawa et al., 2008). Furthermore, chloroplasts were unable to move in response to changes in light intensity. The authors suggested that the presence of the coiled-coil region in the truncated CHUP1–GFP fusion was sufficient to anchor chloroplasts to the plasma membrane on the anticlinal

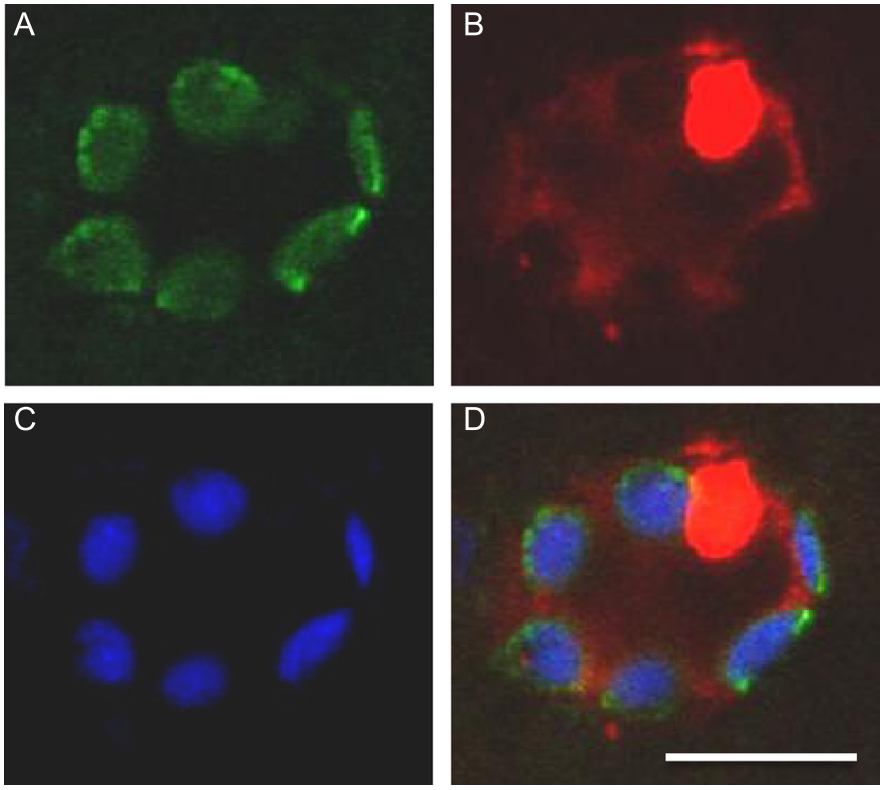

Fig. 5. Colocalization of CaMV P6–RFP with CHUP1$_{FL}$–GFP after particle bombardment of *N. benthamiana* leaves. (A) Expression of CHUP1$_{FL}$–GFP. (B) Expression of P6–RFP. (C) Autoflourescence of chloroplasts. (D) Overlay of panels A–C. Confocal images were taken three days post particle bombardment. Magnification bar in panel (D) is 10 μm.

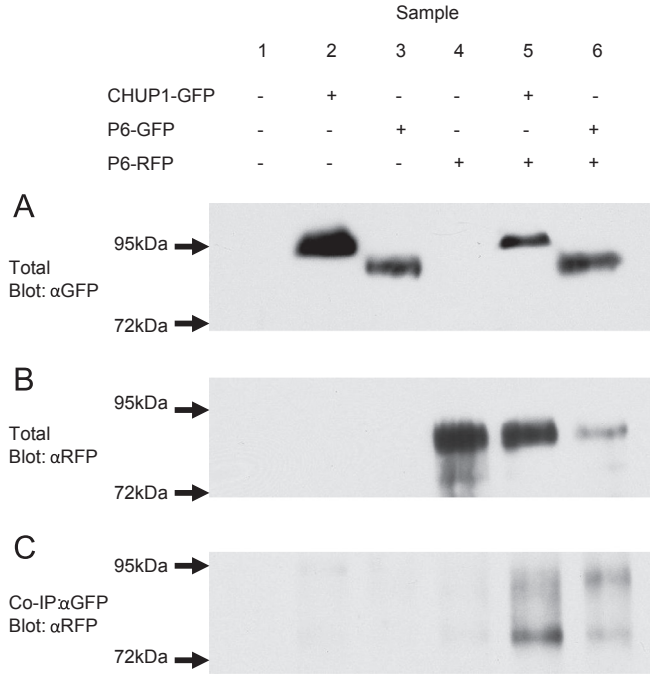

Fig. 6. Co-immunoprecipitation of CaMV P6–RFP by CaMV P6–GFP, and CHUP1$_{436}$–GFP after agroinfiltration of *N. benthamiana* leaves. Lane 1, mock leaf control; Lane 2, Expression of CHUP1$_{436}$–GFP alone; Lane 3, Expression of P6–GFP only; Lane 4, Expression of P6–RFP only; Lane 5, Co-expression of CHUP1$_{436}$–GFP and P6–RFP; Lane 6, Co-expression of P6–GFP and P6–RFP. (A) Western blot for total proteins input probed against GFP antibodies. (B) Western blot for total protein input probed against RFP antibodies. (C) Western blot for immunoprecipitation using GFP antibodies and probed against RFP antibodies. All samples taken were taken at 2–3 dpinf, and co-agroinfiltrated with a construct expressing the TBSV P19 silencing suppressor.

side, but the deletion of the C-terminus abolished chloroplast movement in response to light (Oikawa et al., 2008).

Since our CHUP1$_{436}$–ECFP construct did not contain the domain for chloroplast realignment, but did localize to chloroplasts similarly to the CHUP1$_{1–500}$–GFP construct, we investigated whether its transient overexpression from the 35S promoter might block the movement of P6 IBs due to the absence of the movement domain. Three days after co-agroinfiltration of leaves with P6–Venus and CHUP1$_{436}$–ECFP, P6 IBs were essentially immobilized within cells through our observation period of 295 s (Suppl. Movie 1). By contrast, P6 IBs resulting from agroinfiltration of P6–Venus alone exhibited rapid movement over a distance of 10 μm in *N. benthamiana* cells (Suppl. Movie 2), similar to the results of Harries et al. (2009a). Furthermore, P6–Venus IBs also exhibited comparable movement when co-agroinfiltrated with a binary vector that expressed free ECFP (Suppl. Movie 3). Thus, our work indicated that not only does CHUP1 interact with CaMV P6, but a truncated CHUP1 deficient in chloroplast movement can block the transport of P6 IB-like complexes.

Supplementary material related to this article can be found online at http://dx.doi.org/10.1016/j.virol.2013.05.028.

Silencing CHUP1 slows the rate of CaMV local lesion formation in N. edwardsonii

To investigate whether CHUP1 has a role in CaMV infections, we sought to silence CHUP1 through a virus-induced gene silencing (VIGS) assay in *N. edwardsonii.* As a prelude to investigating the CHUP1 influence on CaMV infections, we first cloned and sequenced the entire *CHUP1* gene from *N. benthamiana* and a portion of the gene from *N. edwardsonii*, both hosts of CaMV. The *N. benthamiana CHUP1* gene (*NbCHUP1*) is 4914 bp in length and encodes nine exons (Suppl. Fig. 3). The encoded amino acid sequences of the *NbCHUP1* and

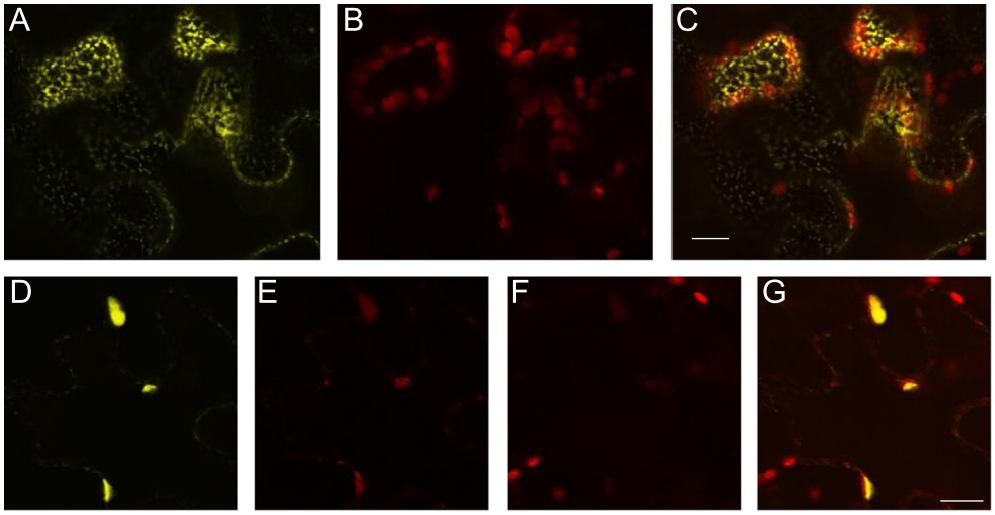

Fig. 7. Colocalization of CaMV P6-RFP with EYFP-CHUP1$_{436}$ in *N. benthamiana* by confocal microscopy. (A) Expression of EYFP-CHUP1$_{436}$. (B) Autofluorescence of chloroplasts present in the image shown in panel A. (C) Overlay of panels A and B. Magnification bar, 10 μm. (D) Expression of EYFP–CHUP1$_{436}$. (E) Expression of P6–RFP in the image shown in panel D. (F) Autofluorescence of chloroplasts present in the image shown in panel D. (G) Overlay of panels D–F. Magnification bar is 10 μm.

AtCHUP1 exons vary in identity from a low of 22% in exon II to a high of 93% in exon VI. The amino acid sequence of the actin-binding domain of NbCHUP1 is identical to AtCHUP1, whereas the N-terminal hydrophobic domain of NbCHUP1, the region responsible for targeting the CHUP1 protein to chloroplasts, is 72% identical with AtCHUP1. The amino acid sequence of the coiled-coil domain responsible for binding AtCHUP1 to P6 is 70% identical with the same region in NbCHUP1 (Suppl. Fig. 4).

To silence *CHUP1* in *Nicotiana* species a 345 bp sequence from *NbCHUP1* exon IV, corresponding to a portion of the coiled-coil domain and the actin binding domain, was inserted into the RNA2 clone of a *Tobacco rattle virus* (TRV) vector (Liu et al., 2002). The nucleotide sequence of this region was 98% identical to corresponding *CHUP1* regions from *N. edwardsonii* (*NeCHUP1*) and *N. tabacum* (*NtCHUP1*) (Suppl. Fig. 5). Silencing of *NeCHUP1* was induced by co-agroinfiltration of the RNA1 and RNA2–CHUP1 clones into young *N. edwardsonii* plants (TRV–CHUP1 plants). Individual leaves were evaluated for silencing of CHUP1 mRNA between 21 and 26 after agroinfiltration. Quantitative RT-PCR assays showed that CHUP1 mRNA in the TRV–CHUP1-infiltrated plants was silenced to approximately 5% the level observed in control plants infiltrated with TRV containing no gene fragment insert (TRV; Fig. 8A).

The silenced and associated control plants were then inoculated with CaMV virions and inoculated leaves were scored for necrotic local lesion numbers daily for a period of up to 19 days. CaMV necrotic local lesions began to form between 9 and 12 (days post-inoculation (dpi), and lesion numbers increased every day thereafter for the next 7–8 days. Mean values for CaMV lesions present on CHUP1-silenced leaves were lower than those from leaves infiltrated with the empty TRV vector, but there was no significant statistical difference observed between treatments through the observation period (Suppl. Fig. 6). We considered that local lesion assays could be confounded due to normal leaf-to-leaf variation for receptivity to virion inoculations and therefore inhibit our ability to identify treatment effects.

To minimize the influence of leaf-to-leaf variation on lesion formation and thereby facilitate comparisons between leaves, the lesion number for individual leaves at 19 dpi was used to approximate the capacity of each leaf for CaMV local lesion formation. By recording local lesion numbers for each leaf at earlier time points, it was possible to determine the rate of local lesion formation over time, expressed each day as a percentage of total lesions formed by 19 dpi. When local lesion numbers were analyzed in this manner, we determined that there was a significant delay in lesion formation from 14–18 dpi (ANOVA, $p=0.01$) (Fig. 8B). The differential effect on local lesion development at later time points was reproduced in three experiments, indicating that silencing of *CHUP1* slowed the CaMV infection process.

Discussion

Here we have shown that the CaMV P6 protein physically interacts with the coiled-coil domain of CHUP1, a plant protein responsible for moving chloroplasts to different regions of the plasma membrane on microfilaments in response to changes in light intensity (Oikawa et al., 2003, 2008). In healthy plants, the coiled-coil domain of CHUP1 functions to anchor the protein and its chloroplast cargo to the plasma membrane (Oikawa et al., 2003, 2008). Under low light conditions, chloroplasts accumulate in palisade cells at the plasma membrane along the periclinal cell wall to optimize photosynthesis. Under high light intensity, chloroplasts move to the anticlinal plasma membrane location to minimize the possibility of damage to their photosynthetic machinery. The association of P6 with CHUP1 may explain a previous observation concerning the localization of P6 IB's with microfilaments (Harries et al., 2009a).

In our assays we did not find strong co-localization between P6 IBs and chloroplasts when P6–GFP, P6–RFP or P6–Venus were agroinfiltrated individually. In CaMV-infected plants, P6 IBs also do not appear to be closely associated with chloroplasts and other host components (Fujisawa et al., 1967; Rubio-Huertos et al., 1968; Shalla et al., 1980). The coiled-coil domain of CHUP1 which binds P6 is also responsible for homo-dimerization of the protein and its interaction with the plasma membrane (Oikawa et al., 2003, 2008; Lehmann et al., 2011). Thus, it may be that native CHUP1 is already bound to chloroplasts and plasma membrane, and amounts synthesized by the plant during the experiment would not be sufficient to significantly draw P6 or P6 IBs into the chloroplast outer membrane or compete with plasma membrane association. In contrast, the co-agroinfiltration of CHUP1$_{436}$–ECFP with P6–Venus would result in *de novo* synthesis of both proteins, and the newly synthesized CHUP1$_{436}$–ECFP therefore was more available to interact with P6–YFP. The ability of both CHUP1 and P6 to, respectively, dimerize and self-interact, may explain (a) our ability

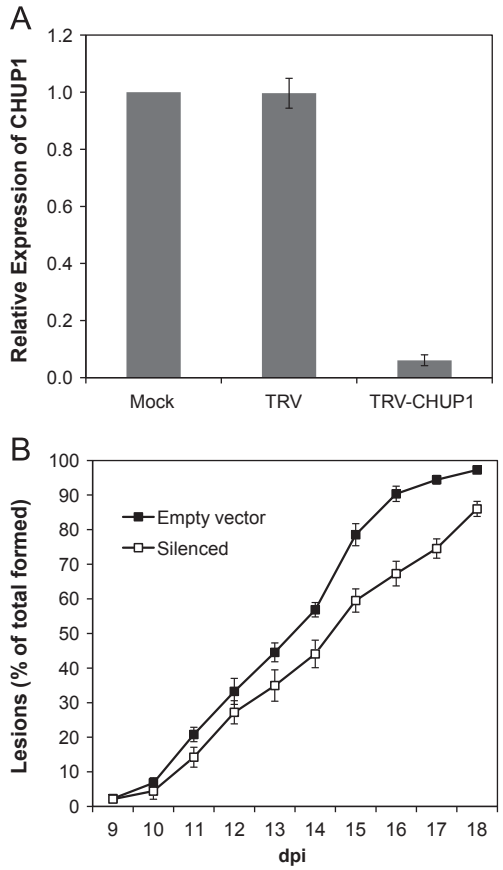

Fig. 8. Silencing CHUP1 in *N. edwardsonii* results in a delay in CaMV lesion formation. (A) Analysis of *CHUP1* mRNA silencing in leaves of *N. edwardsonii* induced through virus-induced gene silencing using a TRV vector. Quantitative RT-PCR analysis was used to determine the relative expression ratio of *CHUP1* in leaves of *N. edwardsonii* inoculated with buffer (Mock), TRV without insert (TRV) and TRV containing a fragment of the *CHUP1* gene (TRV–CHUP1). Error bars illustrate the standard deviation about the mean for three biological replicates for TRV and TRV–CHUP1 treatments. (B) The percentage of total local lesions over time in plants expressing or silenced for *CHUP1* mRNA expression through virus-induced gene silencing. Each value represents the number of local lesions induced by CaMV at that time point divided by the number of local lesions present at the end of the experiment (19 dpi) and reported as a percentage. Each value represents the mean percent of lesions present for single leaves from 10 individual plants inoculated with TRV or single leaves from 11 individual plants inoculated with TRV–CHUP1 +/− standard error. Lesion numbers were obtained from the same plants through the time period. The percentage of total lesions was less in CHUP1 silenced plants using the aggregate value from 14 through 18 dpi for each replicate and comparing between treatments (ANOVA, $p < 0.01$).

to observe co-localization of CHUP1 with two different cargoes, the P6 and chloroplasts and (b) the formation of large aggregates of CHUP1, P6 and chloroplasts. The ability of P6 to compete with plasma membrane for binding to the coiled-coil domain of CHUP1 and the ability of P6 to bind to the coiled-coil domain and still allow CHUP1 dimerization all require further investigation to predict strengths of interactions between these components *in vivo*.

We found that CHUP1 interacted with domain D2 of CaMV P6, and to a lesser extent domain D4 (Figs. 1 and 2). Domain D2 corresponds to the mini-TAV function of P6 (De Tapia et al., 1993; Kobayashi and Hohn, 2004), a function necessary for translation of viral proteins on the polycistronic 35 S RNA. P6 is thought to interact with eIF3g to facilitate translation reinitiation. It may be that domains D2 and D4 facilitate interactions with a variety of host proteins to carry out essential but disparate functions such as viral gene expression and intracellular movement. Kobayashi and Hohn (2004) probed the structure of P6 by making a series of small deletions within P6 and then testing their affect on replication of the virus and infectivity in whole plants. Small deletions within domains D2, D3 or D4 (Fig. 1) abolished replication, with the exception of a pair of small deletions at the C-terminus of P6. Interestingly, small deletions with domain D1 had a minimal effect on replication, but were necessary for efficient CaMV spread in both cruciferous and solanaceous hosts (Kobayashi and Hohn, 2004), providing further evidence that P6 has a role in virus movement. It is tempting to speculate that deletions within D2 might abolish CaMV infection due to lack of TAV function, but that deletions with D1 might affect the structure of P6 to slow the intra- or intercellular movement of the virus.

Although P6 associates with and traffics along microfilaments during its ectopic expression as a GFP fusion (Harries et al., 2009a), the mechanism of the interaction was not determined in that study. CHUP1 is necessary for movement of chloroplasts on microfilaments, and transient expression of a truncated CHUP1 acts as a dominant negative inhibitor of chloroplast movement (Oikawa et al., 2008). Essentially the same truncated CHUP1 construct reported to block chloroplast movement also immobilized P6 IBs when co-agroinfiltrated with the P6 gene (Suppl. Movie 1). This finding may explain the mechanism by which CaMV P6 localizes to microfilaments for movement of IBs within the cell. Specifically, the association of P6, through its D2 domain, with the coiled-coil domain of CHUP1 would allow for self-association of P6 through domain D3 (Li and Leisner, 2002) and/or D1 (Haas et al., 2005) while simultaneously linking IBs to microfilaments or chloroplasts through the actin or chloroplast binding domains of CHUP1 (Fig. 1).

Likewise, our finding that silencing expression of CHUP1 in *N. edwardsonii* inhibited the normal induction of local lesions by CaMV may help to explain a previous observation where treatment of *N. edwardsonii* leaves with latrunculin B, a pharmacological agent that disrupts microfilaments, abolished the development of local lesions by CaMV (Harries et al., 2009a). Here, we now suggest that the interaction of P6 with CHUP1 not only supports transport of ectopically-expressed P6 in the cell, but local virus accumulation and spread, likely including the intracellular transport of P6 IBs to the plasmodesmata.

Several recent studies have shown that plant viruses or host proteins necessary for sustained virus spread utilize the actomyosin system to support virus or virus component movement within the cell (Amari et al., 2011; Avisar et al., 2008; Harries et al., 2009b; Harries et al., 2010; Wei et al., 2010). Plant virus proteins shown to require microfilaments for intracellular movement include the 126-kDa protein of TMV, Hsp70h of BYV, TGBp2 and TGBp3 of potexviruses, and the 6K2 protein of Tobacco etch virus (reviewed in Harries et al., 2010). Two types of experimental approaches have been utilized to implicate myosins in virus or ectopically-expressed virus protein movement; silencing myosins through the use of VIGS (Harries et al., 2009b) and expressing truncated myosins that function as dominant negative inhibitors (Amari et al., 2011; Avisar et al., 2008; Wei et al., 2010). However, no study to date has shown a physical association between a plant virus protein and a myosin or any other motor-like protein.

Here we have shown an interaction between a virus protein, P6, and a plant protein, CHUP1, known to interact with microfilaments. Interestingly, however, our attempt to fully block CaMV systemic accumulation by VIGS of CHUP1 delayed, but did not prevent accumulation (Fig. 8). Although remaining CHUP1 in the plant during VIGS may have been sufficient to allow CaMV accumulation, it also may be that redundancies exist in the plant which support CaMV spread in the absence of CHUP1. In studies of myosin involvement in virus movement, attempts to abolish virus infections by blocking interactions with myosins have only been partially successful. For example, silencing of myosin class XI-2 in

N. benthamiana reduced the size of lesions induced by GFP-tagged TMV, but infection and spread still occurred (Harries et al., 2009b). Similarly, dominant negative inhibition of class XI-K and XI-2 myosins in *N. benthamiana* reduced the size of foci induced by GFP-tagged GFLV but infections were not abolished (Amari et al., 2011). These studies underscore the difficulties in trying to characterize the role of individual plant proteins in intracellular movement of viruses. They demonstrate the involvement of host proteins in movement, but in each case an alternate protein, possibly a second family member or an unrelated protein with functional redundancy, must exist to complement the activity of the plant protein that was silenced. Because CHUP1 is not a member of a multigene family the functional redundancy would necessarily be supplied by a protein with no sequence identity. Myosins could fulfill these requirements and require further study for their involvement in CaMV accumulation and movement.

Methods

Plants and viruses

Seeds of *N. benthamiana* (PI 555478) and *N. edwardsonii* (PI 555704) were obtained from the U.S. Tobacco Germplasm Collection at North Carolina State University (Lewis and Nicholson, 2007). All plants were propagated under greenhouse conditions at the University of Missouri (Columbia, MO). Virions of CaMV W260 strain were purified from turnip infected leaves (*Brassica rapa* subsp. rapa cv. Just Right), according to Schoelz et al. (1986), and mechanically inoculated onto leaves of Arabidopsis or *N. edwardsonii* plants. CaMV experiments with *N. edwardsonii* were conducted in the greenhouse during the months of November through March or in growth chambers set with light intensity of 150 $\mu mol/m^2/s$, 10 h day length, and 19 ± 2 °C (Qiu et al., 1997).

Yeast two-hybrid analysis

Yeast two-hybrid (Y2H) screening was performed by Hybrigenics Services, S.A.S (Paris, France). The coding sequence for the full length CaMV P6 protein was PCR-amplified from plasmid pW260 (Schoelz and Shepherd, 1988) and cloned into pB29 as an N-terminal fusion to LexA (N-P6–LexA-C). The sequence of the entire construct was verified and used as a bait to screen a random-primed *A. thaliana* cDNA library constructed from 1-week old seedlings into pP6 prey vector. pB29 and pP6 are derived from the original pBTM116 (Vojtek and Hollenberg, 1995)and pGADGH (Bartel et al., 1993) plasmids, respectively. Eighty one million clones (8-fold the complexity of the library) were screened using a mating approach with Y187 (mata) and L40ΔGal4 (mata) yeast strains as previously described (Fromont-Racine et al., 1997). Eighty five His+ colonies were selected on a medium lacking tryptophan, leucine and histidine. The prey fragments of the positive clones were amplified by PCR, sequenced at their 5′ and 3′ junctions, and the resulting sequences were used to identify the corresponding interacting proteins in the GenBank database (NCBI).

To identify the domains of P6 that interact with *CHUP1*, a second Y2H assay was performed using only the 363 nt region of *A. thaliana CHUP1* identified in the Hybrigenics Y2H. The region corresponding to positions 489–851 of the CHUP1 coding sequence (Oikawa et al., 2003, AT3G25690) was amplified from *A. thaliana* Col-0 genomic DNA by PCR, with forward and reverse primers containing *Eco*RI and *Xho*I sites, respectively. The PCR product was cloned into pGEM-T easy vector (Promega, Madison WI) for nucleotide sequence confirmation, and subsequently cloned into the yeast plasmid pJG4-5 (Gyuris et al., 1993), a plasmid that contained the activation domain (Li and Leisner, 2002). The four P6 self-association domains were previously cloned into the yeast plasmid pEG202 and the Y2H analysis was performed as described in Li and Leisner (2002). All PCR primers were synthesized by Integrated DNA Technologies (Coralville, IA), and all sequencing reactions were performed at the DNA Core Facility of the University of Missouri (Columbia, MO).

Cloning of A. thaliana CHUP1, eIF3g, and CaMV P6 fused to fluorescent proteins

Total RNA from *A. thaliana* Col-0 was extracted using an RNeasy plant mini kit (Qiagen, Valencia CA), and DNAse treated with Turbo DNA-free (Ambion, Austin TX). cDNA synthesis was done using an Improm-II ™ reverse transcription system kit (Promega, Madison WI), with 15 nt oligo (dt) primers following the manufacturer's instructions. Using this cDNA template, a DNA fragment corresponding to the first 1308 nt of the *CHUP1* coding sequence was amplified by PCR and cloned into a pGEM-T Easy vector (Promega, Madison WI). The nucleotide sequence of the *CHUP1* insert was determined at the DNA Core Facility at the University of Missouri to confirm that no mutations had been introduced during PCR. The 1308 nt *CHUP1* fragment was cloned into pDONR-201 and then cloned into selected pSITE expression vectors (Chakrabarty et al., 2007, Martin et al., 2009), resulting in both N- and C-terminal fusions of a truncated CHUP1 to fluorescent proteins using Gateway Technology ® (Invitrogen, Carlsbad CA), following the manufacturer's instructions. The entire 1560 nt of CaMV gene VI, minus its stop codon, was amplified from the plasmid pW260 (Schoelz and Shepherd, 1988) by PCR and cloned into pDONR-201 vector using Gateway Technology ®. After the gene VI nucleotide sequence was verified, it was cloned into selected pSITE vectors, resulting in the fusion of fluorescent proteins to the C-terminus of P6. For the *eIF3g* gene (AT3G11400), a full-length cDNA clone was obtained from the ABRC, and the coding sequence without its stop codon was cloned into pDONR-201, and then into a pSITE vector, creating a fusion at the C-terminus of eIF3g with Venus. pSITE vectors containing the CHUP1, eIF3g, and P6 sequences were electroporated into *A. tumefaciens* strain AGL-1 (Lazo et al., 1991). Candidate colonies were selected on appropriate antibiotics, and screened for the pSITE clones by colony PCR. To create $CHUP_{154}$–GFP, the PCR primers CHUPF (5′GGGGGAAGCTTCACCATGTTTGTCCGGATAGGGTTT3′) and CHUPR (5′GAAGGTGAATTACTCGAGTATTACGG3′) was used to amplify the first 154 codons of CHUP1 and the PCR product was subsequently cloned into the *Hind*III–*Xho*I sites of pKYLX7–GFP (Angel et al., 2011). This placed the $CHUP_{154}$ coding sequence under the control of the CaMV 35 S promoter and fused it in-frame to the mGFP5 coding sequence (Siemering et al., 1996) (Fig. 1).

Agroinfiltration and biolistic transient expression assays and confocal microscopy

Agrobacterium cultures containing pSITE vectors were agroinfiltrated into leaves of 8–12 weeks old *N. benthamiana* plants as described by Angel et al. (2011). To extend and enhance the transient expression of target proteins, we co-agroinfiltrated an Agrobacterium culture that expressed the *Tomato bushy stunt virus* P19 protein. The *p19* gene had been cloned previously in the *A. tumefaciens* binary vector pKYLX7 (Angel et al., 2011). The final optical density at 600 nm for individual constructs was 0.6–1.0.

For biolistic particle delivery involving $CHUP1_{FL}$–GFP and P6–RFP, we used a PDS-1000/He system (Bio-Rad, Hercules CA), present in the Plant Transformation Core Facility at the University of Missouri. The $CHUP1_{FL}$–GFP and P6–RFP plasmid DNAs were coated onto 0.6 μm gold microcarriers (Bio-Rad, Hercules CA) and shot into detached *N. benthamiana* leaves according to the

manufacturer's protocol. Expression of $CHUP1_{FL}$–GFP and P6–RFP proteins was assessed three days post-bombardment.

Confocal laser scanning microscopy was performed at the University of Missouri Molecular Cytology Core (Columbia, MO), using a Zeiss LSM 510 META microscope, under multitrack mode set with the following parameters for excitation/emission filters wavelengths: 458 nm/480–520 nm for ECFP, 488 nm/501–530 for GFP, 514 nm/535–590 mn for Venus and EYFP, 543 nm/565–615 nm for RFP, and 488 nm or 543 nm/ 650–710 nm for chloroplast auto-fluorescence. *N. benthamiana* leaves were observed between 2 and 4 days postinfiltration (dpinf)for transient expression. Time-lapse images to show movement of P6–Venus inclusion bodies with and without $CHUP1_{436}$–ECFP, were obtained in a Zeiss LSM 5 LIVE line-scanning confocal microscope every 5 s from a single optical plane during 5 minutes. Excitation/emission filters were 488 nm/520–555 nm for Venus (YFP), and 405 nm/445–505 nm for ECFP, respectively. Confocal images were processed using LSM software (Carl Zeiss, Peabody MA), and movies were assembled using ImageJ software (http://imagej.nih.gov/ij).

Co-immunoprecipitation of CaMV P6–RFP with AtCHUP1–EGFP and CaMV P6 EGFP

The co-immunoprecipitations were done according to Lee et al., (2003), with a few modifications. Briefly, *N. benthamiana* plants 6–10 weeks old were agroinfiltrated with the GFP and RFP constructs simultaneously or individually, including the TBSV P19 silencing suppressor. Infiltrated leaf panels were collected at 2–3 dpinf, and ground at 1:2 ratio (wt./vol.) tissue: extraction buffer (25 mM Tris pH 7.5, 150 mM NaCL, 1 mM DTT, 1 mM PMSF, 25 mM Na3VO4, 5 mM NaF, 1X plant proteases inhibitor cocktail (Sigma, St. Louis MO), 1 mM CaCL2, 0.1% Triton X-100, 5% Glycerol, and 0.5% NP40). The extract was filtered through Miracloth and clarified at 2000 g for 10 min at 4 °C. Then, 200–300 μl of extract were pre-cleared with 20–30 μl of packed Protein G-Sepharose beads previously washed (Invitrogen, Frederick, MD). After centrifugation at 2000 *g*, the pellet containing the beads was discarded, and the cleared extract was incubated overnight with 2.0 μg of the polyclonal GFP antibody (Santa Cruz Biotechnology, Santa Cruz, CA), and fresh 20–30 μl of washed-packed Protein G beads. After a brief centrifugation to collect the beads, the pellet was washed 4–5 times with extraction buffer, and then resuspended in 30 μl of 1X loading sample buffer. After boiling for 10 min, the sample was centrifuged to pellet the beads, and the supernatant was collected and run in an 8% SDS-PAGE. Gel proteins from total extracts, pull down assays, and the Co-IPs were transferred to a 0.45 μm nitrocellulose membrane. Western blot analyses were performed incubating the blocked membrane with rabbit-anti-RFP (Invitrogen, Eugene, OR) or goat-anti-GFP (Santa Cruz Biotechnology, Santa Cruz, CA) antibodies at 1: 5000 or 1: 1000 dilutions in 2.5% dry skim milk in TBS–Tween 0.2%. Following several washes, horseradish peroxidase conjugates of goat-anti-rabbit or rabbit-anti-goat antibodies (Sigma, Saint Louis, MO), were used for RFP and GFP blots respectively, at a 1:5000 (vol./vol.) dilution. Finally, the blots were exposed to a chemiluminescent substrate and developed by X-ray autoradiography.

Cloning of N. benthamiana CHUP1 gene, VIGS, and quantitative RT-PCR

To clone the full length *N. benthamiana CHUP1* gene, genomic DNA was extracted as described by Dellaporta et al., 1983, and PCR primers were designed based on mRNA sequences annotated as partial *CHUP1* unigenes from *N. tabacum* (SGN-U447326) and *N. benthamiana* (SGN-U513917), contained at the Sol Genomics Network database (SGN; http://solgenomics.net/, Bombarely et al., 2011). Amplified PCR fragments were purified by agarose gel elution using a QIAquick Gel Extraction kit (Qiagen, Valencia CA), then cloned into the pGEM-T Easy vector (Promega, Madison WI), and candidate clones were submitted for sequencing in both orientations at the DNA Sequencing Core Facility at the University of Missouri (Columbia MO). Sequences were analyzed by BLASTN (Altschul et al., 1997) and Clustal W2 (Larkin et al., 2007), and contigs were assembled manually and using CAP3 (Huang and Madan, 1999).

To target the CHUP1 mRNA for VIGS in *N. edwardsonii*, a 345 bp genomic DNA sequence from exon IV of the *N. benthamiana* and *N. edwardsonii CHUP1* genes (See Supplemental Fig. 5), was amplified by PCR with the forward primer 5′-GAATTCAATTTGAAACATACAAATGAG-3′ and the reverse primer 5′-CTCGAGACTAAATCTGCTTGTGGAACT-3′. The amplified DNA fragment was cloned into the pGEM-T Easy vector and the nucleotide sequence confirmed. Forward and reverse primers contained *Eco*RI and *Xho*I sites respectively to facilitate cloning of the 345 bp *nbCHUP1* sequence into a modified pTRV2 vector (Liu et al., 2002). After the sequences of the clones were verified, the pTRV2–CHUP1 plasmid was electroporated into *A. tumefaciens* AGL-1 cells, and selected colonies were screened for the 345 bp insert by colony PCR. TRV infections were initiated by co-agroinfiltration of the pTRV1 and pTRV2–CHUP1 vectors into leaves of 5–6 weeks old *N. edwardsonii* plants. As a negative control, the pTRV2 empty plasmid vector was co-agroinfiltated with the pTRV1 vector. To further assess the environmental conditions for induction of VIGS, *N. edwardsonii* and *N. benthamiana* plants were agroinoculated with a TRV vector carrying a *phytoene desaturase* (*PDS*) gene sequence (Liu et al., 2002) to induce bleaching of leaves. CaMV was inoculated to CHUP1-silenced and TRV empty vector plants when the entire leaves of PDS-silenced plants exhibited photobleaching.

Partially purified CaMV virions (Schoelz et al., 1986) were mechanically inoculated to the four youngest expanded leaves per plant, 21–24 days after the agroinfiltration of TRV vectors (approximately four leaves above the leaves agroinfiltrated with TRV). The number of necrotic local lesions elicited by CaMV was evaluated every day from their initial formation at approximately 9 dpi until 19 dpi. The progression of local lesion development, expressed as a percentage of daily lesions based on the total number of lesions at 19 dpi per each leaf, was analyzed by the ANOVA.

To confirm silencing of the *CHUP1* transcript in *N. edwardsonii*, quantitative real time PCR (qRT-PCR) was performed on RNA extracted from upper, non-inoculated leaves, collected 24 days after agroinfiltration of the TRV vectors. In addition, samples of comparable leaves from a healthy *N. edwardsonii* plant were included as a negative control. The forward primer NbChup1aF 5′-TGGAACTACTGCTCGGAAAGA-3′ and the reverse primer NbChup1aR 5′-TTGGTTAGCTTCAAGCAGCAT-3′ amplified a 84 nt fragment of the *N. benthamiana CHUP1* exon III. EF-1A was the internal loading control. General procedures for qRT-PCR assays and analysis are described in Harries et al. (2009b).

Acknowledgments

The authors thank Dr. Michael Goodin (University of Kentucky) for the gift of Agrobacterium pSITE expression vectors, and Dr. Sam-Geun Kong (Kyushu University) for the gift of $CHUP1_{FL}$–GFP. We thank Dr. Howard Berg (The Donald W. Danforth Center, St. Louis MO), Dr. Aleksandr Jurkevic and Dr. Zhanyuan Zhang (University of Missouri) for their assistance with confocal microscopy and biolositics. We thank Dr. Malay Saha, Dr. David Pintel, Dr. Shrikesh Sachdev, Dr. Boovaraghan Balaji, Bethany A. Bishop, and Sandra Valdes for technical assistance. This project was supported by the Agriculture and Food Research Initiative Competitive Grants Program no. 2010-65108-20525

from the USDA National Institute of Food and Agriculture and The Samuel Roberts Noble Foundation, Inc.

Appendix A. Supporting information

Supplementary data associated with this article can be found in the online version at http://dx.doi.org/10.1016/j.virol.2013.05.028.

References

Altschul, S.F., Madden, T.L., Schaffer, A.A., Zhang, J., Zhang, Z., Miller, W., Lipman, D.J., 1997. Gapped BLAST and PSI-BLAST: a new generation of protein database search programs. Nucleic Acids Res. 25, 3389–3402.

Amari, K., Lerich, A., Schmitt-Keichinger, C., Dolja, V.V., Ritzenthaler, C., 2011. Tubule-guided cell-to-cell movement of a plant virus requires class XI myosin motors. PLoS Pathog. 7, e1002327.

Angel, C.A., Hsieh, Y-C.H., Schoelz, J.E., 2011. Comparative analysis of the capacity of tombusvirus P22 and P19 proteins to function as avirulence determinants in nicotiana species. Mol. Plant Microbe Interact. 24, 91–99.

Avisar, D., Prokhnevsky, A.I., Dolja, V.V., 2008. Class VIII myosins are required for plasmodesmatal localization of a closterovirus Hsp70 homolog. J. Virol. 82, 2836–2843.

Baird, P.L., Chien, CT., Sternglanz, R., Fields, S., 1999. Circular permutation and receptor insertion within green fluorescent proteins. Proc. Natl. Acad. Sci. U. S. A. 96, 11241–11246.

Bartel, P.L., Chien, C-T., Sternglanz, R., Fields, S., 1993. Using the two-hybrid system to detect protein–protein interactions. In: Hartley, D.A. (Ed.), Cellular Interactions in Development: A Practical Approach. Oxford University Press, Oxford, pp. 153–179.

Baughman, G.A., Jacobs, J.D., Howell, S.H., 1988. *Cauliflower mosaic virus* gene VI produces a symptomatic phenotype in transgenic tobacco plants. Proc. Natl. Acad. Sci. USA 85, 733–737.

Bombarely, A., Menda, N., Tecle, I.Y., Buels, R.M., Strickler, S., Fischer-York, T., et al., 2011. The sol genomics network (solgenomics.net): growing tomatoes using Perl. Nucleic Acids Res. 39, D1149–D1155.

Bureau, M., Leh, V., Haas, M., Geldreich, A., Ryabova, L., Yot, P., Keller, M., 2004. P6 protein of *Cauliflower mosaic virus*, a translational reinitiator, interacts with ribosomal protein L13 from *Arabidopsis thaliana*. J. Gen. Virol. 85, 3765–3775.

Campbell, R.E., Tour, O., Palmer, A.E., Steinbach, P.A., Baird, G.S., Zacharias, D.A., Tsien, R.Y., 2004. A monomeric red fluorescent protein. Proc. Natl. Acad. Sci. USA 99, 7877–7882.

Chakrabarty, R., Banerjee, R., Chung, S.M., Farman, M., Citovsky, V., Hogenhout, S.A., Tzfira, T, Goodin, M., 2007. pSITE vectors for stable integration or transient expression of autofluorescent protein fusions in plants: probing *Nicotiana benthamiana*-virus interactions. Mol. Plant-Microbe Interact. 20, 740–750.

Conti, G.G., Vegetti, G., Bassi, M., Favali, M.A., 1972. Some ultrastructural and cytochemical observations on chinese cabbage leaves infected with *Cauliflower mosaic virus*. Virology 47, 694–700.

Daubert, S.D., Schoelz, J., Debao, L., Shepherd, R.J., 1984. Expression of disease symptoms in *Cauliflower mosaic virus* genomic hybrids. J. Mol. Appl. Genet. 2, 537–547.

Dellaporta, S.L., Wood, J.W., Hicks, J.B., 1983. A plant DNA minipreparation: Version II. Plant Mol. Biol. Rep. 1, 19–21.

De Tapia, M., Himmelbach, A., Hohn, T., 1993. Molecular dissection of the *Cauliflower mosaic virus* translation transactivator. EMBO J. 12, 3305–3314.

Fromont-Racine, M., Rain, J.C., Legrain, P., 1997. Toward a functional analysis of the yeast genome through exhaustive two-hybrid screens. Nat. Genet. 16, 277–282.

Fujisawa, I., Rubio-Huertos, M., Matsui, C., Yamaguchi, A., 1967. Intracellular appearance of *Cauliflower mosaic virus* particles. Phytopathology 57, 1130–1132.

Gyuris, J., Golemis, E., Chertkov, H., Brent, R., 1993. Cdi1, a human G1 and S phase protein phosphatase that associates with Cdk2. Cell 75, 791–803.

Haas, M., Azevedo, J., Moissiard, G., Geldreich, A., Himber, C., Bureau, M., Fukuhara, T., Keller, M., Voinnet, O., 2008. Nuclear import of CaMV P6 is required for infection and suppression of the RNA silencing factor DRB4. EMBO J. 6, 2102–2112.

Haas, M., Geldreich, A., Bureau, M., Dupuis, L., Leh, V., Vetter, G., Kobayashi, K., Hohn, T., Ryabova, L., Yot, P., Keller, M., 2005. The open reading frame VI product of *Cauliflower mosaic virus* is a nucleocytoplasmic protein: its N terminus mediates its nuclear export and formation of electron-dense viroplasms. Plant Cell 17, 927–943.

Hapiak, M., Li, Y.Z., Agama, K., Swade, S., Okenka, G., Falk, J., Khandekar, S., Raikhy, G., Anderson, A., Pollock, J., Zellner, W., Schoelz, J., Leisner, S.M., 2008. *Cauliflower mosaic virus* gene VI product N-terminus contains regions involved in resistance-breakage, self-association and interactions with movement protein. Virus Res. 138, 119–129.

Harries, P., Palanichelvam, K., Yu, W., Schoelz, J.E., Nelson, R.S., 2009a. The *Cauliflower mosaic virus* protein P6 forms motile inclusions that traffic along actin microfilaments and stabilize microtubules. Plant Physiol. 149, 1005–1016.

Harries, P.A., Park, J-W., Sasaki, N., Ballard, K.D., Maule, A.J., Nelson, R.S., 2009b. Differing requirements for actin and myosin by plant viruses for sustained intercellular movement. Proc. Natl. Acad. Sci. USA 106, 17594–17599.

Harries, P.A., Schoelz, J.E., Nelson, R.S., 2010. Intracellular transport of viruses and their components: Utilizing the cytoskeleton and membrane highways. Mol. Plant-Microbe Interact. 23, 1381–1393.

Heim, R., Tsien, R.Y., 1996. Engineering green fluorescent protein for improved brightness, longer wavelengths and fluorescence energy transfer. Curr. Biol. 6, 178–182.

Himmelbach, A., Chapdelaine, Y., Hohn, T., 1996. Interaction between *Cauliflower mosaic virus* inclusion body protein and capsid protein: implications for viral assembly. Virology 217, 147–157.

Hohn, T., Fütterer, J., 1997. The proteins and functions of plant pararetroviruses: knowns and unknowns. Crit. Rev. Plant Sci. 16, 133–167.

Huang, X., Madan, A., 1999. CAP3: a DNA sequence assembly program. Genome Res. 9, 868–877.

Kasteel, D.T.J., Perbal, M.C., Boyer, J.C., Wellink, J., Goldbach, R.W., Maule, A.J., van Lent, J.W.M., 1996. The movement proteins of cowpea mosaic virus and *Cauliflower mosaic virus* induce tubular structures in plant and insect cells. J. Gen. Virol. 77, 2857–2864.

Kobayashi, K., Hohn, T., 2004. The avirulence domain of *Cauliflower mosaic virus* translactivator/viroplasmin is a determinant of viral virulence in susceptible hosts. Mol. Plant Microbe Interact. 17, 475–483.

Larkin, M.A., Blackshields, G., Brown, N.P., Chenna, R., McGettigan, P.A., McWilliam, H., Valentin, F., Wallace, I.M., Wilm, A., Lopez, R., Thompson, J.D., Gibson, T.J., Higgins, D.G., 2007. Clustal W and Clustal X version 2.0. Bioinformatics 23, 2947–2948.

Lazo, G.R., Stein, P.A., Ludwig, R.A., 1991. A DNA transformation-competent Arabidopsis genomic library in Agrobacterium. BioTechnology 9, 963–967.

Leclerc, D., Burri, L., Kajava, A.V., Mougeot, J.L., Hess, D., Lustig, A., Kleemann, G., Hohn, T., 1998. The open reading frame III product of *Cauliflower mosaic virus* forms a tetramer through a N-terminal coiled-coil. J. Biol. Chem. 273, 29015–29021.

Leclerc, D., Stavolone, L., Meier, E., Guerra-Peraza, O., Herzog, E., Hohn, T., 2001. The product of ORF III in *Cauliflower mosaic virus* interacts with the viral coat protein through its C-terminal proline rich domain. Virus Genes 22, 159–165.

Lee, S.S., Cho, H.S., Yoon, G.M., Ahn, J.W., Kim, H.H., Pai, H.S., 2003. Interaction of NtCDPK1 calcium-dependent protein kinase with NtRpn3 regulatory subunit of the 26S proteasome in *Nicotiana tabacum*. Plant J. 33, 825–840.

Leh, V., Yot, P., Keller, M, 2000. The *Cauliflower mosaic virus* translational transactivator interacts with the 60 S ribosomal subunit protein L18 of *Arabidopsis thaliana*. Virology 266, 1–7.

Lehmann, P., Bohnsack, M.T., Schleiff, E., 2011. The functional domains of the chloroplast unusual positioning protein 1. Plant Sci. 180, 650–654.

Lewis, R.S., Nicholson, J.S., 2007. Aspects of the evolution of *Nicotiana tabacum* L. and the status of the United States *Nicotiana* germplasm collection. Genet. Resour. Crop Evol. 54, 727–740.

Li, Y., Leisner, S.M., 2002. Multiple domains within the *Cauliflower mosaic virus* gene VI product interact with the full-length protein. Mol. Plant Microbe Interact. 15, 1050–1057.

Liu, Y., Schiff, M., Dinesh-Kumar, S.P., 2002. Virus-induced gene silencing in tomato. Plant J. 31, 777–786.

Love, A.J., Laird, J., Holt, J., Hamilton, A.J., Sadanandom, A., Milner, J.J., 2007. *Cauliflower mosaic virus* protein P6 is a suppressor of RNA silencing. J. Gen. Virol. 88, 3439–3444.

Love, A.J., Geri, C., Laird, J., Carr, C., Yun, B-W., Loake, G.J., Tada, Y., Sasanandom, A., Milner, J.J., 2012. *Cauliflower mosaic virus* protein P6 inhibits signaling responses to salicylic acid and regulates innate immunity. PLoS ONE 7 (10), e47535, doi: 10. 1371/journal.pone.0047535.

Lutz, L., Raikhy, G., Leisner, S.M., 2012. *Cauliflower mosaic virus* major inclusion body protein interacts with the aphid transmission factor, the virion-associated protein, and gene VII product. Virus Res. 170, 150–153.

Martin, K., Kopperud, K., Chakrabarty, R., Banerjee, R., Brooks, R., Goodin, M.M., 2009. Transient expression in *Nicotiana benthamiana* fluorescent marker lines provides enhanced definition of protein localization, movement and interactions in planta. Plant J. 59, 150–162.

Nagai, T., Ibata, K., Park, E.S., Kubota, M., Mikoshiba, K., Miyawaki, A, 2002. A variant of yellow fluorescent protein with fast and efficient maturation for cell-biological applications. Nat. Biotechnol. 20, 87–90.

Odell, J.T., Howell, S.H., 1980. The identification, mapping, and characterization of mRNA for P66, a *Cauliflower mosaic virus*-coded protein. Virology 102, 349–359.

Oikawa, K., Kasahara, M., Kiyosue, T., Kagawa, T., Suetsugu, N., Takahashi, F., Kanegae, T., Niwa, Y., Kadota, A., Wada, M., 2003. Chloroplast unusual positioning 1 is essential for proper chloroplast positioning. Plant Cell 15, 2805–2815.

Oikawa, K., Yamasato, A., Kong, S-G., Kasahara, M., Nakai, M., Takahashi, F., Ogura, Y., Kagawa, T., Wada, M., 2008. Chloroplast outer envelope protein CHUP1 is essential for chloroplast anchorage to the plasma membrane and chloroplast movement. Plant Phys. 148, 829–842.

Park, H-S., Himmelbach, A., Browning, K.S., Hohn, T., Ryabova, L.A., 2001. A plant viral "reinitiation" factor interacts with the host translational machinery. Cell 106, 723–733.

Perbal, M.C., Thomas, C.L., Maule, A.J., 1993. *Cauliflower mosaic virus* gene-I product (P1) forms tubular structures which extend from the surface of infected protoplasts. Virology 195, 281–285.

Qiu, S.G., Wintermantel, W.M., Sha, Y., Schoelz, J.E., 1997. Light-dependent systemic infection of solanaceous species by *Cauliflower mosaic virus* can be conditioned by a viral gene encoding an aphid transmission factor. Virology 227, 180–188.

Rubio-Huertos, M., Matsui, C., Yamaguchi, A., Kamei, T., 1968. Electron microscopy of X-body formation in cells of cabbage infected with Brassica virus 3. Phytopathology 58, 548–549.
Ryabova, L.A., Pooggin, M.M., Hohn, T., 2002. Viral strategies of translation initiation: ribosomal shunt and reinitiation. Prog. Nucleic Acid Res. Mol. Biol. 72, 1–39.
Schmidt von Braun, S., Schleiff, E., 2008. The chloroplast outer membrane protein CHUP1 interacts with actin and profilin. Planta 227, 1151–1159.
Schoelz, J.E., Harries, P.A., Nelson, R.S., 2011. Intracellular transport of plant viruses: finding the door out of the cell. Mol. Plant 4, 813–831.
Schoelz, J.E., Shepherd, R.J., 1988. Host range control of *Cauliflower mosaic virus*. Virology 162, 30–37.
Schoelz, J.E., Shepherd, R.J., Daubert, S.D., 1986. Gene VI of CaMV encodes a host range determinant. Mol. Cell. Biol. 6, 2632–2637.
Shalla, T.A., Shephered, R.J., Peterson, L.J., 1980. Comparative cytology of nine isolates of *Cauliflower mosaic virus*. Virology 102, 381–388.
Shockey, M.W., Gardner Jr., C.O., Melcher, U., Essenberg, R.C., 1980. Polypeptides associated with inclusion bodies from leaves of turnip infected with *Cauliflower mosaic virus*. Virology 105, 575–581.
Siemering, K.R., Golbik, R., Sever, R., Haseloff, J., 1996. Mutations that suppress the thermosensitivity of green fluorescent protein. Curr. Biol. 6, 1653–1663.
Stavolone, L., Villani, M.E., Leclerc, D., Hohn, T., 2005. A coiled-coil interaction mediates *Cauliflower mosaic virus* cell-to-cell movement. Proc. Natl. Acad. Sci. USA 102, 6219–6224.
Vojtek, A., Hollenberg, S.M., 1995. Ras-Raf interaction: two-hybrid analysis. Methods Enzymol. 255, 331–342.
Wei, T., Huang, T-S., McNeil, J., Laliberté, J-F., Hong, J., Nelson, R.S., Wang, A., 2010. Sequential recruitment of the endoplasmic reticulum and chloroplasts for plant potyvirus replication. J. Virol. 84, 799–809.
Wintermantel, W.M., Anderson, E.J., Schoelz, J.E., 1993. Identification of domains within gene VI of *Cauliflower mosaic virus* that influence systemic infection of Nicotiana bigelovii in a light-dependent manner. Virology 196, 789–798.
Yu, W., Murfett, J., Schoelz, J.E., 2003. Differential induction of symptoms in Arabidopsis by P6 of *Cauliflower mosaic virus*. Mol. Plant Microbe Interact. 16, 35–42.